

# Optimal singular value shrinkage with noise homogenization

William Leeb\* and Elad Romanov†

## Abstract

We derive the optimal singular values for prediction in the spiked model with noise homogenization, which equalizes the noise level across all coordinates. As part of this derivation, we obtain new asymptotic results for the high-dimensional spiked model with heteroskedastic noise, and consistent estimators for the relevant population parameters. We demonstrate the advantages of noise homogenization theoretically and through simulations. Specifically, we prove that in a certain asymptotic regime optimal shrinkage with homogenization converges to the best linear predictor, whereas shrinkage without homogenization converges to a suboptimal linear filter. We show that homogenization increases a natural signal-to-noise ratio of the observations. We also extend previous analysis on out-of-sample prediction to the setting of predictors with homogenization.

## 1 Introduction

Singular value shrinkage is a popular method for denoising data matrices. It is performed by computing a singular value decomposition of the observed matrix  $Y$ , adjusting the singular values, and reconstructing. The idea is that when  $Y = X + N$ , where  $X$  is a low-rank signal matrix we wish to estimate, the additive noise term  $N$  inflates the singular values of  $X$ ; by shrinking them we can move the estimated matrix closer to  $X$ , even if the singular vectors remain inaccurate. Much work has been done in the past several years on deriving optimal singular value shrinkage methods (and the related problem of eigenvalue shrinkage for covariance estimation) [28, 15, 26, 13, 14, 12], and applying them to various scientific problems [6, 2, 25].

This paper is concerned specifically with the *spiked model* [19]. Here, the observation matrix is composed of iid columns  $Y_i$  in  $\mathbb{R}^p$ ,  $i = 1, \dots, n$  from some distribution consisting of signal vectors  $X_i$  lying on a low-dimensional subspace, plus independent noise vectors  $\varepsilon_i$  with some covariance matrix  $\Sigma_\varepsilon$ . The theory for prediction of  $X_1, \dots, X_n$  in the spiked model with orthogonally invariant noise, i.e. when  $\Sigma_\varepsilon = \sigma^2 I$ , is largely complete [13, 28, 15]. Singular value shrinkage is known to be minimax optimal, and asymptotically optimal shrinkers have been derived for a wide variety of loss functions.

However, since it is rare to encounter orthogonally invariant noise in applications, a natural question is what procedure to use when  $\Sigma_\varepsilon$  is not a multiple of the identity; that is, when the noise is *heteroskedastic*. The paper [26] derives optimal singular value shrinkers for general noise matrices, so long as the singular vectors of the signal the noise matrices are sufficiently incoherent with respect to each other. Other recent work on PCA with heteroskedastic noise includes [33].

In this paper, we take a different approach to the setting of non-isotropic noise. We study the procedure dubbed *homogenization* in the paper [23]. Our version of homogenization is as follows. We first estimate the noise covariance matrix  $\Sigma_\varepsilon$ . We then normalize, or *homogenize*, the observations  $Y_i$  by applying  $\Sigma_\varepsilon^{-1/2}$ ; the resulting vectors  $Y_i^h$  consist of a transformed signal component  $X_i^h = \Sigma_\varepsilon^{-1/2} X_i$ , plus *isotropic* noise  $G_i = \Sigma_\varepsilon^{-1/2} \varepsilon_i$ . Singular value shrinkage is then performed on this new, homogenized observation matrix, after which the inverse transformation  $\Sigma_\varepsilon^{1/2}$  is applied.

While the applicability of this approach is restricted to cases when  $\Sigma_\varepsilon$  can be consistently estimated, when it does apply there are a number of advantages of the procedure over the method described in [26]. First, in the classical “large  $n$ ” asymptotic limit our method is equivalent to the optimal linear predictor of the data, an oracle method that requires knowledge of the population principal components. By contrast, singular value shrinkage without homogenization is equivalent to a strictly suboptimal linear filter. Further, we show that homogenization transfers energy from the noise matrix to the signal matrix, and improves the estimation of the population singular vectors. Next, because we perform shrinkage on a matrix with isotropic noise, we impose weaker assumptions on the principal components of the signal

\*School of Mathematics, University of Minnesota, Twin Cities, Minneapolis, MN, USA.

†School of Computer Science and Engineering, The Hebrew University, Jerusalem, Israel.

vectors. Finally, the computational load of our method is lighter, as we require computation of only the dominant singular vectors and values of the homogenized observation matrix, and not the full singular value spectrum.

We must emphasize that the procedure we describe is *not* a singular value shrinkage predictor; that is, it is not equivalent to performing singular value shrinkage to the data matrix  $Y$ . However, the middle step of our procedure does perform singular value shrinkage to the homogenized matrix  $Y^h$ , and the question then arises: what are the optimal singular values to use? While homogenization has been used with shrinkage in previous works, it appears that this question has never been addressed, and suboptimal singular values have always been employed. In this paper, we derive the precise choice of optimal singular values, and show, using new asymptotic results, how to consistently estimate them from the observed data.

## 1.1 The observation model

We now specify the particular model we will be studying in this paper. We observe iid vectors  $Y_1, \dots, Y_n$  in  $\mathbb{R}^p$ , of the form:

$$Y_i = X_i + \varepsilon_i, \quad (1)$$

where

$$X_i = \sum_{k=1}^r \ell_k^{1/2} z_{ik} u_k \quad (2)$$

is a low-rank signal with random  $z_{ik}$  satisfying  $\mathbb{E}z_{ik} = 0$  and  $\text{Var}(z_{ik}) = 1$ ; and

$$\varepsilon_i = \Sigma_\varepsilon^{1/2} G_i \quad (3)$$

is a Gaussian noise vector with covariance  $\Sigma_\varepsilon$ , i.e. the entries of  $G_i = (g_{i1}, \dots, g_{ip})^\top$  are iid  $N(0, 1)$ . The noise vectors  $G_i$  are drawn independently from the  $z_{ik}$ 's. We note now that the assumption that  $X_i$  has mean zero is not essential; all the results of this paper will go through with almost without modification if we first estimate the mean of  $X$  by the sample mean and subtract it from each observation  $Y_i$ . The vectors  $u_k$  are called the *principal components (PCs)* of the random vector  $X$ . For simplicity, we will assume that  $X_i$  is subgaussian, i.e. that the  $z_{ik}$ 's are subgaussian random variables; again, this assumption is made for convenience only, and can certainly be relaxed.

As we are primarily interested in the high-dimensional setting for this problem, we will let the number of variables  $p = p_n$  grow with  $n$ . Specifically, we will assume that the limit

$$\gamma = \lim_{n \rightarrow \infty} \frac{p_n}{n} \quad (4)$$

is well-defined and finite.

We impose a certain *incoherence* assumption relating the noise covariances  $\Sigma_\varepsilon$  and the principal components of the signal,  $u_k$ . Specifically, we will assume that:

$$\lim_{p \rightarrow \infty} u_j^\top \Sigma_\varepsilon^{-1} u_k = \begin{cases} 0, & \text{if } j \neq k \\ \tau_k, & \text{if } j = k \end{cases}, \quad (5)$$

where  $\tau_k$  is a finite, positive value, unknown a priori. We assume that the spectrum of  $\Sigma_\varepsilon$  stays bounded between  $a_{\min} > 0$  and  $a_{\max} < \infty$ .

The assumption (5) is significantly weaker than assumptions in related works [26, 10]. For example, it will hold if the entries of  $u_k$  are drawn iid from a fixed distribution, or if the entries are independently drawn with differing variances (for example,  $u_k = Dw_k / \|Dw_k\|$ , where the entries of  $w_k$  are iid and  $D$  is a diagonal matrix of bounded operator norm); this can include the case where a fixed proportion of entries of  $u_k$  are deterministically set to zero. Another example is if the matrix  $\Sigma_\varepsilon$  is diagonal and the vectors  $u_k$  have disjoint supports.

Finally, in order to have well-defined asymptotics in the large  $p$ , large  $n$  regime, we will assume that the normalized trace of  $\Sigma_\varepsilon$  has a well-defined limit, which we will denote by  $\mu_\varepsilon$ :

$$\mu_\varepsilon = \lim_{p \rightarrow \infty} \frac{\text{tr}(\Sigma_\varepsilon)}{p} \in (0, \infty). \quad (6)$$

Our task is to obtain a prediction for the signal vectors  $X_i$ , or equivalently the normalized signal matrix  $X = [X_1, \dots, X_n]/\sqrt{n}$ . Throughout, we will use the asymptotic mean squared error to measure the accuracy of an estimator  $\hat{X}$ :

$$\text{AMSE} = \lim_{n \rightarrow \infty} \mathbb{E} \|\hat{X} - X\|_F^2 = \lim_{n \rightarrow \infty} \frac{1}{n} \sum_{i=1}^n \|\hat{X}_i - X_i\|^2 \quad (7)$$

We will denote the normalized observed matrix by  $Y = [Y_1, \dots, Y_n]/\sqrt{n}$ , and the normalized noise matrices by  $G = [G_1, \dots, G_n]/\sqrt{n}$  and  $N = [\varepsilon_1, \dots, \varepsilon_n]/\sqrt{n} = \Sigma_\varepsilon^{1/2} G$ .

## 1.2 Singular value shrinkage

A standard method for predicting the matrix  $X$  from the observed matrix  $Y$  is known as *singular value shrinkage*. We will define singular value shrinkage in detail in Section 2.2. Briefly, it is performed by leaving fixed the singular vectors of  $Y$ , while adjusting its singular values. The idea is to deflate the empirical singular values to remove the effects of noise.

More precisely, if the singular value decomposition of  $Y$  is given by  $Y = \hat{U} \cdot \hat{\Lambda} \cdot \hat{V}^\top$ , then  $\hat{X}$  is given by:

$$\hat{X} = \hat{U} \cdot \hat{S} \cdot \hat{V}^\top \quad (8)$$

where  $\hat{S}$  is a diagonal matrix. It is shown in [13] that when the noise matrix  $N$  is just white Gaussian noise, or in other words  $\Sigma_\varepsilon = I_p$ , then singular value shrinkage is minimax optimal for predicting  $X$  from  $Y$ .

In [15], the optimal singular value shrinkers are derived for isotropic (but not necessarily Gaussian) noise for a large family of loss functions, not just the Frobenius norm loss we consider in this paper. The effectiveness of this method rests on the asymptotic spectral theory of the data matrix  $Y$  developed in [27, 5] among others.

In the paper [26], the optimal singular value shrinker (known as ‘OptShrink’) is derived under much more general conditions on the noise matrix  $N$ , by exploiting the general asymptotic spectral theory developed in [5] for non-isotropic noise. While OptShrink may be effectively applied when the noise is non-isotropic, it then requires the signal principal components to be essentially random.

## 1.3 Shrinkage with noise homogenization

In this paper, we will consider a procedure related to shrinkage, but with a crucial difference. Rather than perform the singular value decomposition of the raw data  $Y$ , we first perform a change of variables to *homogenize* the noise,  $\varepsilon_i$ . Specifically, we replace the observations  $Y_i$  with the homogenized observations

$$Y_i^h = H X_i + H \varepsilon_i = X_i^h + G_i, \quad (9)$$

where  $H = \Sigma_\varepsilon^{-1/2}$  is the *homogenization transformation*. In Section 3.3 we will discuss the estimation of  $H$  when it is not available a priori. The vectors  $Y_i^h$  are still of the form ‘‘low rank plus noise’’, but the noise term has been transformed into an isotropic Gaussian.

We then perform singular value shrinkage on the matrix  $Y^h = [Y_1^h, \dots, Y_n^h]$ . More precisely, if  $\hat{u}_1^h, \dots, \hat{u}_r^h$  and  $\hat{v}_1, \dots, \hat{v}_r$  are the top left and right, respectively, singular vectors of  $Y^h$ , then we define

$$\hat{X}^h = \sum_{k=1}^r s_k \cdot \hat{u}_k^h \cdot \hat{v}_k^\top \quad (10)$$

for singular values  $s_k$  which we will determine.  $\hat{X}^h$  is a predictor of the transformed matrix  $X^h$ ; so we arrive at a predictor for  $X$  itself by applying the inverse change of variables  $H^{-1}$ . That is, we define our predictor of  $X$  to be:

$$\hat{X} = \sum_{k=1}^r s_k \cdot H^{-1} \hat{u}_k^h \cdot \hat{v}_k^\top. \quad (11)$$

This three-step procedure (homogenize, shrink, unhomogenize) depends on the choice of singular values  $s_k$  used in the middle step. As we will show, it turns out that it is possible to consistently estimate the optimal singular values  $s_k$ . We will present this derivation in Section 3.2.

## 1.4 Why homogenize the noise?

In addition to deriving the optimal shrinker for homogenization, in this paper we also present several arguments why homogenization is expected to outperform shrinkage. In Section 4, we show that in the  $\gamma = 0$  regime, shrinkage with homogenization converges to the optimal linear predictor of the data, while shrinkage without homogenization will converge to a different, typically suboptimal, linear filter. In that sense, not only is shrinkage with homogenization preferable to no homogenization, but the homogenization transform is the optimal change of coordinates to apply to the data before shrinking.

In Section 3, we present a different argument, applicable in the  $\gamma > 0$  regime, suggesting that homogenization is beneficial. Specifically, we show that a natural notion of the “signal-to-noise” ratio is larger for the homogenized matrix  $Y^h$  than for the raw data matrix  $Y$ . This result is similar in spirit to one found in [23], though we use a different, and we believe more appropriate, definition of SNR.

Finally, in Section 6 we show numerical evidence in favor of homogenization, namely that it outperforms optimal shrinkage without homogenization for prediction problems. As part of this demonstration, we show that homogenization produces empirical singular vectors that are better correlated with the population singular vectors than are the singular vectors of the raw data, and that homogenization can cause signal components that are buried in the noise to “pop out” and become detectable.

## 1.5 Related work and our contributions

A number of previous papers have designed optimal singular value shrinkage procedures for matrices in the low-rank spiked model in high dimensions, under slightly different modeling assumptions. For matrices with additive isotropic Gaussian noise, the paper [28] designed asymptotically optimal singular value shrinkers for the Frobenius loss, while [15] designed optimal singular value shrinkers for isotropic Gaussian noise for a much larger class of orthogonally invariant loss functions. The paper [26] designed optimal shrinkers for a very broad range of noise distributions. We will review the essential elements of these works in Section 2.

The homogenization procedure we describe in this work can be seen as an example of what is called *weighted PCA*, in which weights are applied to individual variables before the principal components are computed [20, 18]. The inverse standard deviation of the noise, as we advocate in this work, is a standard choice of weights [30, 32, 31]; in that sense, the present work can be seen as providing a theoretical justification for this already widely-used choice.

For the specific task of prediction in the spiked model with heteroskedastic noise, previous works have proposed pairing the homogenization transformation with singular value shrinkage. The paper [23] proposes the use of homogenization in conjunction with exponential family noise models. The paper [10] proposes homogenization in the context of transformed spiked models. The paper [6] also uses homogenization in the context of covariance estimation.

However, in the aforementioned previous works a suboptimal choice of singular value shrinker was employed. More precisely, the values  $s_k$  used do not minimize the Frobenius loss between  $\hat{X}$  and  $X$ . In this paper, we show how to derive explicit, estimable formulas for the optimal  $s_k$ . These formulas are based on deriving asymptotic limits for the angles between the population singular vectors and the empirical singular vectors that arise after homogenization. Like those in the spiked model with isotropic noise, the new limiting formulas we derive are simple, algebraic expressions that can be consistently estimated from the observed data itself.

Furthermore, we also present a new understanding of shrinkage procedures by explicitly relating them to linear predictors. More precisely, we show that singular value shrinkage converges in the  $\gamma = 0$  limit to a linear filter of the data, and singular value shrinkage with homogenization converges to the optimal linear filter. The underlying reason for this is that the  $\gamma = 0$  regime, the empirical principal components converge to the eigenvectors of the sum of the signal and noise covariance matrices. In general, these matrices will not commute, and their eigenvectors are therefore not the true principal components of the  $X_i$ . However, after the homogenization procedure the noise covariance is the identity matrix, which commutes with the transformed signal covariance and thereby ensures consistent estimation of the population principal components. This analysis is performed in Section 4. As part of the same framework, in Section 5 we extend results from [10] on the *out-of-sample* prediction problem, where the singular vectors from an initial pool of data are used to denoise an independent, out-of-sample observation.

In Section 3 we also present new results on the benefits of homogenization in high dimensions ( $\gamma > 0$ ). Specifically, we show that homogenization increases a notion of the operator norm signal-to-noise ratio (SNR); this is similar in spirit to a result in [23], which used a different notion of SNR based on Frobenius

norms. As we explain in Section 3.5, we believe that the operator norm SNR we employ in this paper is more natural for the high-dimensional setting. We supplement these results with numerical experiments in Section 6 that illustrate our theory and demonstrate the benefits of homogenization.

## 2 Preliminaries

In this section, we will review known results on the asymptotic spectral theory of the spiked model and singular value shrinkage. This will also serve to introduce notation we will use throughout the text.

### 2.1 Asymptotic spectral theory of the spiked model

The spectral theory of the observed matrix  $Y$  has been thoroughly studied in the large  $p$ , large  $n$  regime, when  $p = p_n$  grows with  $n$ . We will offer a brief survey of the relevant results from the literature [27, 5, 10].

In the case of isotropic Gaussian noise (that is, when  $\Sigma_\varepsilon = I_p$ ), the  $r$  largest singular values of the matrix  $Y$  converge to  $\lambda_k$ , defined by:

$$\lambda_k^2 = \begin{cases} (\ell_k + 1)(1 + \gamma/\ell_k), & \text{if } \ell_k > \sqrt{\gamma}, \\ (1 + \sqrt{\gamma})^2, & \text{if } \ell_k \leq \sqrt{\gamma}. \end{cases} \quad (12)$$

Furthermore, the top singular vectors  $\hat{u}_k^y$  and  $\hat{v}_k^y$  of  $Y$  make asymptotically deterministic angles with the singular vectors  $u_k$  and  $v_k$  of  $X$ . More precisely, the absolute cosines  $|\langle \hat{u}_j^y, u_k \rangle|$  converge to  $c_k = c_k(\gamma, \ell_k)$ , defined by

$$c_k^2 = \begin{cases} \frac{1 - \gamma/\ell^2}{1 + \gamma/\ell} & \text{if } j = k \text{ and } \ell_k > \sqrt{\gamma}, \\ 0 & \text{otherwise} \end{cases}, \quad (13)$$

and the absolute cosines  $|\langle \hat{v}_j^y, v_k \rangle|$  converge to  $\tilde{c}_k = \tilde{c}_k(\gamma, \ell_k)$ , defined by

$$\tilde{c}_k^2 = \begin{cases} \frac{1 - \gamma/\ell^2}{1 + 1/\ell} & \text{if } j = k \text{ and } \ell_k > \sqrt{\gamma}, \\ 0 & \text{otherwise} \end{cases}. \quad (14)$$

We note that when  $\ell_k > \sqrt{\gamma}$ , the map  $\ell_k \mapsto \lambda_k$  is invertible, implying that the population variances  $\ell_k$  can be estimated from the observed data. Since  $c_k$  and  $\tilde{c}_k$  are functions of  $\ell_k$  and the aspect ratio  $\gamma$ , these quantities can then also be estimated.

The papers [5, 10] derive the asymptotics for more general noise matrices  $N$ . The formulas are defined in terms of the Stieltjes transform [3] of the asymptotic distribution of singular values of  $Y$ , which can be estimated consistently using the observed singular values of  $Y$ , albeit at greater computational cost as a full SVD is required instead of computation of just the top  $r$  singular values.

### 2.2 Optimal shrinkage with Frobenius loss

We defined the class of shrinkage estimators in Section 1.2. We will now review the theory of shrinkage with respect to Frobenius loss; we briefly mention that the paper [15] extends these ideas to a much wider range of loss functions for the spiked model.

We suppose that our predictor of  $X$  is a rank  $r$  matrix of the form

$$\hat{X} = \sum_{k=1}^r t_k \cdot \hat{u}_k \cdot \hat{v}_k^\top, \quad (15)$$

where  $\hat{u}_k$  and  $\hat{v}_k$  are estimated vectors. We will assume that the vectors  $\hat{v}_k$  are orthogonal, and that their cosines with the population vectors  $v_k$  of  $X$  are asymptotically deterministic. More precisely, we assume that  $\langle v_j, \hat{v}_k \rangle^2 \rightarrow \tilde{c}_k^2$  when  $j = k$ , and converges to 0 when  $j \neq k$ . Similarly, we will assume that  $\langle u_j, \hat{u}_k \rangle^2 \rightarrow c_k^2$  when  $j = k$ , and converges to 0 when  $j \neq k$ ; however, we do not need to assume that the  $\hat{u}_k$ 's are orthogonal for the purposes of this derivation.

Expanding the squared Frobenius loss between  $\hat{X}$  and  $X$  and using orthogonality, we get:

$$\begin{aligned}\|\hat{X} - X\|_F^2 &= \left\| \sum_{k=1}^r \left( t_k \hat{u}_k \hat{v}_k^\top - \ell_k^{1/2} u_k v_k^\top \right) \right\|_F^2 \\ &= \sum_{k=1}^r \left\| t_k \hat{u}_k \hat{v}_k^\top - \ell_k^{1/2} u_k v_k^\top \right\|_F^2 + \sum_{j \neq k} \left\langle t_j \hat{u}_j \hat{v}_j^\top - \ell_j^{1/2} u_j v_j^\top, t_k \hat{u}_k \hat{v}_k^\top - \ell_k^{1/2} u_k v_k^\top \right\rangle \\ &\sim \sum_{k=1}^r \left\| t_k \hat{u}_k \hat{v}_k^\top - \ell_k^{1/2} u_k v_k^\top \right\|_F^2.\end{aligned}\tag{16}$$

Since the loss separates over the different components, we may consider each component separately. Using the asymptotic cosines, we have:

$$\left\| t_k \hat{u}_k \hat{v}_k^\top - \ell_k^{1/2} u_k v_k^\top \right\|_F^2 \sim t_k^2 + \ell_k - 2\ell_k^{1/2} c_k \tilde{c}_k t_k,\tag{17}$$

which is minimized by taking

$$t_k = \ell_k^{1/2} c_k \tilde{c}_k.\tag{18}$$

These values of  $t_k$ , therefore, are the optimal ones for estimating  $X$  in Frobenius loss.

Furthermore, we can also derive an estimable formula for the AMSE. Indeed, plugging in  $t_k = \ell_k^{1/2} c_k \tilde{c}_k$  to (17), we get:

$$\text{AMSE} = \sum_{k=1}^r \ell_k^2 (1 - c_k^2 \tilde{c}_k^2).\tag{19}$$

Note that this derivation of the optimal  $t_k$  and the AMSE does not require the vectors  $\hat{u}_k$  and  $\hat{v}_k$  to be the singular vectors of  $Y$ . Rather, we just require the asymptotic cosines to be well-defined. However, to be able to implement this procedure, estimates of  $\ell_k$ ,  $c_k$  and  $\tilde{c}_k$  must be available.

### 3 Optimal shrinkage with homogenization in high dimensions

In this section, we will derive the optimal singular values to be used with the homogenization procedure in the high-dimensional limit  $p/n \rightarrow \gamma > 0$ . We will denote by  $\hat{u}_k^h$  and  $\hat{v}_k$ ,  $k = 1, \dots, r$ , the top  $r$  singular vectors of the matrix  $Y^h = HY$ . Shrinking this matrix, we obtain a matrix of the form

$$\hat{X}^h = \sum_{k=1}^r s_k \cdot \hat{u}_k^h \cdot \hat{v}_k^\top,\tag{20}$$

where  $s_k$  are the shrunken singular values, to be determined. After unhomogenizing, our final predictor is of the form:

$$\hat{X} = \sum_{k=1}^r s_k \cdot H^{-1} \hat{u}_k^h \cdot \hat{v}_k^\top.\tag{21}$$

Our goal is to determine the values  $s_k$  that minimize the AMSE between  $\hat{X}$  and  $X$ , and also to estimate the optimal AMSE.

Defining the unit vectors  $\hat{u}_k$  by

$$\hat{u}_k = \frac{\Sigma_\varepsilon^{1/2} \hat{u}_k^h}{\|\Sigma_\varepsilon^{1/2} \hat{u}_k^h\|},\tag{22}$$

and the scalars  $t_k$  by

$$t_k = s_k \|\Sigma_\varepsilon^{1/2} \hat{u}_k^h\|,\tag{23}$$

we can write  $\hat{X}$  as:

$$\hat{X} = \sum_{k=1}^r t_k \cdot \hat{u}_k \cdot \hat{v}_k^\top.\tag{24}$$

Since  $\|\Sigma_\varepsilon^{1/2}\hat{u}_k^h\|$  is observed, finding the optimal singular values  $s_k$  of  $\hat{X}^h$  is equivalent to finding the optimal coefficients  $t_k$ . This can be done using the framework described in Section 2.2. The resulting method is summarized in Algorithm 1.

We will formally derive this procedure in Section 3.2. Before doing so, however, we need to first understand the asymptotic behavior of the homogenized data matrix. We develop the necessary results in Section 3.1.

---

**Algorithm 1** Optimal shrinkage with noise homogenization

---

- 1: **Input:** observations  $Y_1, \dots, Y_n$ ; noise covariance  $\Sigma_\varepsilon$ ; rank  $r$
  - 2: **Define**  $Y = [Y_1, \dots, Y_n]/\sqrt{n}$ ;  $H = \Sigma_\varepsilon^{-1/2}$ ;  $Y^h = HY$
  - 3: **Compute** rank  $r$  SVD of  $Y^h$ :  $\hat{u}_1^h, \dots, \hat{u}_r^h$ ;  $\hat{v}_1^h, \dots, \hat{v}_r^h$ ;  $\lambda_1^h, \dots, \lambda_r^h$
  - 4: **for all**  $k = 1, \dots, r$  **do**
  - 5:   **if**  $\lambda_k^h > 1 + \sqrt{\gamma}$  **then**

$$\ell_k^h = \left[ (\lambda_k^h)^2 - 1 - \gamma + \sqrt{((\lambda_k^h)^2 - 1 - \gamma)^2 - 4\gamma} \right] / 2$$

$$c_k^h = \sqrt{(1 - \gamma/(\ell_k^h)^2) / (1 + \gamma/\ell_k^h)}$$

$$s_k^h = \sqrt{1 - (c_k^h)^2}$$

$$\tilde{c}_k = \sqrt{(1 - \gamma/(\ell_k^h)^2) / (1 + 1/\ell_k^h)}$$

$$\mu_\varepsilon = \text{tr}(\Sigma_\varepsilon)/p$$

$$\tau_k = (c_k^h)^2 / \left[ \|\Sigma_\varepsilon^{1/2}\hat{u}_k^h\|^2 - (s_k^h)^2\mu_\varepsilon \right]$$

$$s_k = (\ell_k^h)^{1/2} c_k^h \tilde{c}_k / [(c_k^h)^2 + (s_k^h)^2\mu_\varepsilon\tau_k]$$
  - 6:   **else if**  $\lambda_k^h \leq 1 + \sqrt{\gamma}$  **then**

$$s_k = 0$$
  - 7: **Output:**  $\hat{X} = \sum_{k=1}^r s_k (H^{-1}\hat{u}_k^h)(\hat{v}_k^h)^T$
- 

### 3.1 The asymptotics when $\gamma > 0$

We define  $\ell_k^h = \ell_k \cdot \tau_k$ , and define  $c_k^h > 0$  by:

$$(c_k^h)^2 = \begin{cases} \frac{1 - \gamma/(\ell_k^h)^2}{1 + \gamma/\ell_k^h} & \text{if } j = k \text{ and } \ell_k^h > \sqrt{\gamma} \\ 0 & \text{otherwise} \end{cases}, \quad (25)$$

and let  $s_k^h = \sqrt{1 - (c_k^h)^2}$ .

We also define:

$$\tilde{c}_k^2 = \begin{cases} \frac{1 - \gamma/(\ell_k^h)^2}{1 + 1/\ell_k^h} & \text{if } j = k \text{ and } \ell_k^h > \sqrt{\gamma} \\ 0 & \text{otherwise} \end{cases}, \quad (26)$$

and  $\tilde{s}_k = \sqrt{1 - \tilde{c}_k^2}$ .

Because of the incoherence condition (5), the vectors  $u_k^h$  are asymptotically pairwise orthogonal. Consequently, the following result follows immediately from [27, 5]:

**Proposition 3.1.** *If  $p/n \rightarrow \gamma > 0$  as  $n \rightarrow \infty$ , the  $k^{\text{th}}$  largest singular value of  $Y^h$  converges almost surely to*

$$\lambda_k^h = \begin{cases} \sqrt{(\ell_k^h + 1) \left(1 + \frac{\gamma}{\ell_k^h}\right)} & \text{if } \ell_k^h > \sqrt{\gamma} \\ 1 + \sqrt{\gamma} & \text{otherwise} \end{cases}. \quad (27)$$

Furthermore, we have the almost sure limits:

$$\langle u_k^h, \hat{u}_k^h \rangle^2 \rightarrow (c_k^h)^2, \quad \langle v_k, \hat{v}_k \rangle^2 \rightarrow \tilde{c}_k^2. \quad (28)$$

We now derive an asymptotic formula for  $\|\Sigma_\varepsilon^{1/2}\hat{u}_k^h\|$ . While this quantity is directly estimable from the observations, this formula will later be used to derive an estimate for the parameters  $\tau_k$ .

**Proposition 3.2.** *If  $p/n \rightarrow \gamma > 0$  as  $n \rightarrow \infty$ , we have the almost sure limit:*

$$\lim_{p \rightarrow \infty} \|\Sigma_\varepsilon^{1/2}\hat{u}_k^h\|^2 = \frac{(c_k^h)^2}{\tau_k} + (s_k^h)^2 \mu_\varepsilon. \quad (29)$$

*Proof.* Because the noise  $G$  is Gaussian, we can write:

$$\hat{u}_k^h \sim c_k^h u_k^h + s_k^h \tilde{u}_k^h, \quad (30)$$

where  $\tilde{u}_k^h$  is a random unit vector, uniformly random over the sphere in the subspace orthogonal to  $u_1^h, \dots, u_r^h$  (see [27]). Since

$$u_k^h = \frac{H u_k}{\|H u_k\|} \sim \frac{\Sigma_\varepsilon^{-1/2} u_k}{\sqrt{\tau_k}}, \quad (31)$$

we then have:

$$\Sigma_\varepsilon^{1/2} \hat{u}_k^h \sim c_k^h \frac{u_k}{\sqrt{\tau_k}} + s_k^h \Sigma_\varepsilon^{1/2} \tilde{u}_k^h, \quad (32)$$

Taking the squared norm of each side, we obtain:

$$\|\Sigma_\varepsilon^{1/2} \hat{u}_k^h\|^2 \sim \frac{(c_k^h)^2}{\tau_k} + (s_k^h)^2 \|\Sigma_\varepsilon^{1/2} \tilde{u}_k^h\|^2 \sim \frac{(c_k^h)^2}{\tau_k} + (s_k^h)^2 \mu_\varepsilon, \quad (33)$$

where we have used the asymptotic approximation  $\|\Sigma_\varepsilon^{1/2} \tilde{u}_k^h\|^2 \sim \text{tr}(\Sigma_\varepsilon)/p$  (see, e.g., [4]). This completes the proof.  $\square$

The next result characterizes the angles of  $\hat{u}_k$  with the population principal components  $u_j$ .

**Proposition 3.3.** *If  $p/n \rightarrow \gamma > 0$  as  $n \rightarrow \infty$ , we have the almost sure limit:*

$$\langle u_j, \hat{u}_k \rangle^2 \rightarrow c_{jk}^2 = \begin{cases} \frac{(c_k^h)^2}{(c_k^h)^2 + (s_k^h)^2 \mu_\varepsilon \tau_k} & \text{if } j = k \text{ and } \ell_k^h > \sqrt{\gamma}; \\ 0, & \text{otherwise} \end{cases}. \quad (34)$$

*Proof.* As in the proof of Proposition 3.2, we have:

$$\Sigma_\varepsilon^{1/2} \hat{u}_k^h \sim c_k^h \frac{u_k}{\sqrt{\tau_k}} + s_k^h \Sigma_\varepsilon^{1/2} \tilde{u}_k^h, \quad (35)$$

where  $\tilde{u}_k^h$  is a random unit vector, uniformly random over the sphere in the subspace orthogonal to  $u_1^h, \dots, u_r^h$ . Taking inner products with  $u_k$  we get:

$$\langle u_k, \Sigma_\varepsilon^{1/2} \hat{u}_k^h \rangle \sim \frac{c_k^h}{\sqrt{\tau_k}} + s_k^h (u_k^\top \Sigma_\varepsilon^{1/2} \tilde{u}_k^h) \sim \frac{c_k^h}{\sqrt{\tau_k}}, \quad (36)$$

where we have used the randomness of  $\tilde{u}_k^h$ . Consequently, from Proposition 3.2 we have:

$$\langle u_k, \hat{u}_k \rangle^2 \sim \frac{(c_k^h)^2}{\tau_k} \left( \frac{(c_k^h)^2}{\tau_k} + (s_k^h)^2 \mu_\varepsilon \right)^{-1} = \frac{(c_k^h)^2}{(c_k^h)^2 + (s_k^h)^2 \mu_\varepsilon \tau_k}, \quad (37)$$

which shows the claim when  $j = k$ .

When  $j \neq k$ , we take inner products with  $u_j$ . From the orthogonality of  $u_k$  and  $u_j$ , and the randomness of  $\tilde{u}_k^h$  (see [4]), we get:

$$\langle u_j, \Sigma_\varepsilon^{1/2} \hat{u}_k^h \rangle \sim 0, \quad (38)$$

which completes the proof.  $\square$



### 3.2 Deriving the optimal $s_k$ when $\gamma > 0$

From Section 3.1, the cosines of the angles between  $u_k$  and  $\hat{u}_k$  are  $c_k$ , while the cosines of the angles between  $v_j$  and  $\hat{v}_k$  are  $\tilde{c}_k$  when  $j = k$  and 0 otherwise. Consequently, from Section 2.2 we know that the optimal choice of  $t_k$  to minimize the AMSE is

$$t_k = \ell_k^{1/2} c_k \tilde{c}_k. \quad (39)$$

Consequently, the optimal choice of singular values  $s_k$  is:

$$s_k = \frac{\ell_k^{1/2} c_k \tilde{c}_k}{\|\Sigma_\varepsilon^{1/2} \hat{u}_k^h\|}. \quad (40)$$

For this choice of singular values to define a valid estimator, we must show how to estimate the values  $\ell_k$ ,  $c_k$  and  $\tilde{c}_k$  from the observed data itself.

To that end, from Proposition 3.1  $\ell_k^h$  can be estimated by

$$\ell_k^h = \frac{(\lambda_k^h)^2 - 1 - \gamma + \sqrt{((\lambda_k^h)^2 - 1 - \gamma)^2 - 4\gamma}}{2} \quad (41)$$

where  $\lambda_k^h$  is the  $k^{\text{th}}$  singular value of  $Y^h$ . The cosines  $c_k^h$  and  $\tilde{c}_k$  can then be estimated by formulas (25) and (26).

Now, rearranging the result of Proposition 3.2, we can solve for  $\tau_k$  in terms of the estimable quantities  $c_k^h$ ,  $s_k^h$ ,  $\mu_\varepsilon$  and  $\|\Sigma_\varepsilon^{1/2} \hat{u}_k^h\|^2$ :

$$\tau_k \sim \frac{(c_k^h)^2}{\|\Sigma_\varepsilon^{1/2} \hat{u}_k^h\|^2 - (s_k^h)^2 \mu_\varepsilon}. \quad (42)$$

Indeed, this quantity can be estimated consistently:  $c_k^h$  and  $s_k^h$  are estimable from (25),  $\|\Sigma_\varepsilon^{1/2} \hat{u}_k^h\|^2$  is directly observed, and  $\mu_\varepsilon \sim \text{tr}(\Sigma_\varepsilon)/p$ .

Having estimated  $\tau_k$ , we use the formula

$$\ell_k = \frac{\ell_k^h}{\tau_k} \quad (43)$$

to define our estimator of  $\ell_k$ .

Next, we must estimate the cosine  $c_k$ . We already have an estimate of the cosine  $c_k^h$ , and the parameters  $\tau_k$  and value  $\mu_\varepsilon$ . We then need only to apply the formula (34) for  $c_k$ .

This completes the derivation of the optimal shrinker. The entire procedure is described in Algorithm 1.

### 3.3 Estimating the noise covariance $\Sigma_\varepsilon$

Applying the homogenization transformation  $H = \Sigma_\varepsilon^{-1/2}$  requires estimation of the noise covariance matrix  $\Sigma_\varepsilon$ . In certain applications, estimates of  $\Sigma_\varepsilon$  may be available from measurements of pure noise [1], which can be formed prior to processing the observed  $Y_i$ 's. In this section, however, we show how the homogenization transformation may be consistently estimated with some additional domain knowledge.

Specifically, we will assume that we know the basis diagonalizing  $\Sigma_\varepsilon$ . This assumption is often met in practice. For instance, in many imaging applications the noise is assumed to be stationary, i.e. diagonalized by the Fourier basis [1, 2]. Since we know the basis, we will assume without loss of generality that  $\Sigma_\varepsilon$  is diagonal. Let's denote the variance of the  $i^{\text{th}}$  coordinate of the noise,  $\varepsilon_{ij}$ , by  $\sigma_i^2$ .

We will also impose the weak assumption that the  $u_k$ 's are delocalized. More precisely, for each PC  $u_k$ , we will assume that  $\|u_k\|_\infty \rightarrow 0$  as  $p \rightarrow \infty$ . This assumption is much weaker than those in other works [26, 10]. Because in the spiked model the size of the noise dominates the size of the signal, the sample variance of each coordinate will converge almost surely to the variance of the noise in that coordinate; that is, for  $i = 1, \dots, p$ , we have:

$$\hat{\sigma}_i^2 = \frac{1}{n} \sum_{j=1}^n Y_{ij}^2 = \frac{1}{n} \sum_{j=1}^n \left( \sum_{k=1}^r \ell_k u_{ki} z_{jk} \right)^2 + \frac{1}{n} \sum_{j=1}^n \varepsilon_{ij}^2 + 2 \frac{1}{n} \sum_{j=1}^n \varepsilon_{ij} \sum_{k=1}^r \ell_k u_{ki} z_{jk} \rightarrow \sigma_i^2, \quad (44)$$

where the limit is almost sure as  $p, n \rightarrow \infty$ . We have made use of the strong law of large numbers and the almost sure limit  $\|u_k\|_\infty \rightarrow 0$ .

Let  $\hat{\Sigma}_\varepsilon$  be the estimated  $\Sigma_\varepsilon$ , whose  $i^{\text{th}}$  diagonal entry is the sample variance of the  $i^{\text{th}}$  coordinate of the observations,  $\hat{\sigma}_i^2$ . Then  $\hat{\Sigma}_\varepsilon^{1/2} - \Sigma_\varepsilon^{1/2}$  is a mean-zero diagonal matrix, with diagonal entries  $\hat{\sigma}_i - \sigma_i$ ; and the operator norm  $\|\hat{\Sigma}_\varepsilon^{1/2} - \Sigma_\varepsilon^{1/2}\|_{op} = \max_{1 \leq i \leq p} |\hat{\sigma}_i - \sigma_i|$ , which can easily be shown to go to 0 almost surely as  $p \rightarrow \infty$  using the subgaussianity of the observations (in fact, much weaker assumptions suffice, e.g. more than four finite moments). Defining  $\hat{H} = \hat{\Sigma}_\varepsilon^{-1/2}$ , since the minimum variance  $\min_{1 \leq i \leq p} \sigma_i^2$  is uniformly bounded away from 0, it follows that  $\|\hat{H} - H\|_{op} \rightarrow 0$  almost surely too.

Because  $\hat{H}$  approximates  $H$  in operator norm, and  $\hat{\Sigma}_\varepsilon^{1/2}$  approximates  $\Sigma_\varepsilon^{1/2}$  in operator norm, the asymptotic angles and singular values derived in Section 3.1 are still applicable with  $\hat{H}$  and  $\hat{\Sigma}_\varepsilon^{1/2}$  in place of, respectively,  $H$  and  $\Sigma_\varepsilon^{1/2}$ .

### 3.4 Estimating the rank $r$

Our method also assumes knowledge of the rank  $r$  of the signal. A popular method for rank estimation for data in the spiked model with isotropic noise can be found in [22]. Another widely-used method that deals directly with non-isotropic noise is known as *parallel analysis* [17, 8, 7], which has been the subject of recent investigation [9, 11]. Other methods have also been explored [21].

Most rank estimation methods in the spiked model measure the number of singular values of the noisy observed matrix that exceed the bulk edge of the singular value distribution of the pure noise matrix. In the setting of this paper, where the noise covariance  $\Sigma_\varepsilon$  is assumed to be known (or estimable), estimating the bulk edge of the noise can be performed consistently by, for example, simulating Gaussian noise matrices with the specified covariance. The rank of the signal in the observations can then be taken as the number of singular values exceeding the estimated bulk edge of the noise.

Of course, after homogenization, the resulting matrix  $Y^h = X^h + G$  has an isotropic noise component, and the asymptotic bulk edge of the noise is known to be  $1 + \sqrt{\gamma}$ . In principle, we could estimate  $r$  as the number of singular values of  $Y^h$  exceeding this threshold. Since the noise is now isotropic, we can also manage finite sample fluctuations by employing the method of [22].

A natural question is whether the rank estimation is best performed on the original, unhomogenized matrix  $Y$ , or on the homogenized matrix  $Y^h$ . In Section 6.4, we present numerical evidence that homogenization increases the gap between the smallest signal singular value and the bulk edge of the noise, making detection of the signal more reliable.

### 3.5 Homogenization increases the operator norm SNR

In this section, we define a natural notion of signal-to-noise ratio (SNR) for this problem setting, namely the ratio of operator norms between the signal and noise components. We then show that under a generic model for the signal principal components  $u_k$ , namely that they have iid entries, the SNR increases after homogenization is performed.

This is similar in spirit to a result in [23], which essentially shows that the SNR defined by the Frobenius norms increases after homogenization. However, in the spiked model defining the SNR using the ratio of Frobenius norms is not as meaningful as using operator norms, because the ratio of Frobenius norms always converges to 0 in the high-dimensional limit. Indeed, if we let  $\|\cdot\|_F$  denote the Frobenius norm of a matrix and  $\|\cdot\|$  the operator norm. We then have:

$$\|X\|_F^2 \rightarrow \sum_{i=1}^r \ell_i, \quad (45)$$

almost surely as  $p, n \rightarrow \infty$ . On the other hand, it is easy to check that for the noise we have

$$\frac{1}{p} \|N\|_F^2 \rightarrow \mu_\varepsilon. \quad (46)$$

In particular, the Frobenius norm of  $N$  grows like  $\sqrt{p}$ , whereas the Frobenius norm of  $X$  stays fixed. So when  $p$  is large, the norm of the noise swamps the norm of the signal.

On the other hand, the operator norms of  $X$  and  $N$  are both bounded, and may therefore be comparable in size. We therefore define a reasonable measure of “signal-to-noise ratio” as the ratio of operator norms. We will show that the homogenization procedure increases the ratio of the signal operator norm to the noise operator norm.

If there is one spike  $\ell$ , define the SNR by:

$$\text{SNR} = \frac{\|X\|_{op}^2}{\|N\|_{op}^2} \sim \frac{\ell}{\|N\|_{op}^2}, \quad (47)$$

that is, the squared ratio of the signal operator norm to the noise operator norm. If there are  $r$  spikes, then we can define the SNR for each spike individually. That is, we write  $X = \sum_{k=1}^r \ell_k^{1/2} u_k v_k^\top$ , and define:

$$\text{SNR}_k = \frac{\ell_k}{\|N\|_{op}^2}, \quad (48)$$

which is the asymptotic ratio of the squared operator norm of each component  $\ell_k^{1/2} u_k v_k^\top$  of  $X$  and the operator norm of the noise.

After homogenization, the observation changes into:

$$Y^h = X^h + G, \quad (49)$$

where  $X^h$  is still rank  $r$ , and in 1-1 correspondence with  $X$ . Therefore, the new SNR is:

$$\text{SNR}_k^h = \frac{\ell_k^h}{\|G\|_{op}^2} \sim \frac{\ell_k^h}{(1 + \sqrt{\gamma})^2}. \quad (50)$$

We will prove the following:

**Proposition 3.4.** *Suppose the population principal components  $u_1, \dots, u_r \in \mathbb{R}^p$  all have entries that are drawn iid from a fixed distribution with mean zero and variance  $1/p$ . Then in the limit  $p/n \rightarrow \gamma > 0$ ,*

$$\text{SNR}_k^h \leq \text{SNR}_k, \quad (51)$$

with equality holding if and only if  $\Sigma_\varepsilon = \sigma^2 I$  for some  $\sigma > 0$ .

In other words, for generic signals homogenization increases the operator norm SNR.

*Proof.* To show the increase in SNR after homogenization, we will first derive a lower bound on the operator norm of the noise matrix  $N$  alone. Recall that  $N = \Sigma_\varepsilon^{1/2} G$ , where  $g_{ij}$  are iid  $N(0, 1/n)$ .

Take unit vectors  $c$  and  $d$  so that  $Gd = \|G\|_{op} c$ . Then we have

$$\|N\|_{op}^2 \geq \|\Sigma_\varepsilon^{1/2} Gd\|^2 = \|G\|_{op}^2 \|\Sigma_\varepsilon^{1/2} c\|^2 \quad (52)$$

Since the distribution of  $G$  is orthogonally invariant, the distributions of  $c$  is uniform over the unit sphere in  $\mathbb{R}^n$ . Consequently,  $\|\Sigma_\varepsilon^{1/2} c\|^2 \sim \text{tr}(\Sigma_\varepsilon)/p \sim \mu_\varepsilon$ . Therefore,

$$\|N\|_{op}^2 \gtrsim \mu_\varepsilon \cdot \|G\|_{op}^2 \sim \mu_\varepsilon \cdot (1 + \sqrt{\gamma})^2, \quad (53)$$

where “ $\gtrsim$ ” indicates that the inequality holds almost surely in the large  $p$ , large  $n$  limit.

Next, we make use of our assumption in this section that the entries of  $u_k$  are drawn iid from a distribution with variance  $1/p$ . Under this “strongly generic” model, the parameters  $\tau_k$  are asymptotically given by:

$$\tau_k \sim \|\Sigma_\varepsilon^{-1/2} u_k\|^2 \sim \frac{\text{tr}(\Sigma_\varepsilon)}{p}. \quad (54)$$

In particular, unless  $\Sigma_\varepsilon$  is a multiple of the identity, by Jensen’s inequality we have:

$$\frac{1}{\mu_\varepsilon} \sim \frac{1}{\text{tr}(\Sigma_\varepsilon)/p} < \frac{\text{tr}(\Sigma_\varepsilon)}{p} \sim \tau_k. \quad (55)$$

With this, we can show the improvement in SNR after homogenization. We have:

$$\text{SNR}_k = \frac{\ell_k}{\|N\|_{op}^2} \lesssim \frac{\ell_k}{\mu_\varepsilon \cdot (1 + \sqrt{\gamma})^2} < \frac{\ell_k \cdot \tau_k}{(1 + \sqrt{\gamma})^2} = \frac{\ell_k^h}{\|G\|_{op}^2} \sim \text{SNR}_k^h. \quad (56)$$

This completes the proof.  $\square$

### 3.6 Additional advantages of homogenization

We discuss some additional advantages of shrinkage with homogenization over shrinkage of the raw data matrix  $Y$ . The asymptotic spectral theory used to derive optimal shrinkers in [26] requires a strong incoherence between the signal and noise matrices. Specifically, if the noise matrix is not orthogonally invariant, then the signal singular vectors are assumed to be completely random.

In the homogenization approach, however, we are able to get away with less restrictive assumptions on the signal components. This is because homogenization converts the original noise matrix  $N = \Sigma^{1/2}G$  into the orthogonally-invariant noise matrix  $G$ . Consequently, the asymptotic spectral theory for  $X^h + G$  requires no assumptions on the singular vectors of  $X^h$ .

Further, because there are closed, algebraic formulas for the asymptotic cosines and singular values, our method only requires computing the top  $r$  singular values of the homogenized matrix. This can be done efficiently using, for example, the Lanczos method [16]. By contrast, estimating the integral transforms that appear in [26] will typically require computation of the full singular value spectrum of  $Y$ .

## 4 Singular value shrinkage and linear prediction

In this section, we will show a relationship between singular value shrinkage applied with any transformation  $S$  and linear prediction of the vectors  $X_i$ . Specifically, in Section 4.1, we show how both ordinary shrinkage and the three-step procedure from Section 3.2 (homogenization, shrinkage, and unhomogenization) can be written in terms of the individual columns  $X_i$ . In Section 4.2, we then show that in the  $\gamma = 0$  limit, the homogenization procedure converges to the best linear predictor of  $X_i$ , while ordinary shrinkage without homogenization converges to a suboptimal linear filter. In other words, in the  $\gamma = 0$  limit, shrinkage with homogenization is strictly better than shrinkage without homogenization.

We consider the following class of predictors, which subsumes both ordinary singular value shrinkage and singular value shrinkage with noise homogenization. For a fixed matrix  $Q$ , we multiply  $Y$  by  $Q$ , forming the matrix  $Y^q = [QY_1, \dots, QY_n]/\sqrt{n}$ . We then apply shrinkage to this matrix, with singular values  $s_1^q, \dots, s_r^q$ , after which we apply  $Q^{-1}$ . Clearly, ordinary shrinkage is the case when  $Q = I_p$ , whereas singular value shrinkage with homogenization is the cases when  $Q = H = \Sigma_\varepsilon^{-1/2}$ .

When the singular values  $s_1^q, \dots, s_r^q$  are chosen optimally, we will call the resulting predictor  $\hat{X}_Q$ . In this notation,  $\hat{X} = \hat{X}_H$  is shrinkage with homogenization, whereas  $\hat{X}_I$  is ordinary shrinkage without homogenization. All of these predictors can be seen as instances of *weighted principal component analysis*, where the weights are defined by the matrix  $Q$ . The natural question is, what is the optimal matrix  $Q$ ? We will show that in the classical  $\gamma = 0$  asymptotic regime, the optimal choice is  $Q = H$ , the homogenization transformation.

### 4.1 Singular value shrinkage expressed column-wise

In this section, we show how to write the predictor  $\hat{X}_Q$  in terms of the individual columns of  $Y^q = [QY_1, \dots, QY_n]/\sqrt{n}$ . Let  $m = \min(p, n)$ . Consistent with our previous notation, we will denote by  $\hat{u}_1^q, \dots, \hat{u}_m^q$  the left singular vectors of the matrix  $Y^q$ , and we will denote by  $\hat{v}_1^q, \dots, \hat{v}_m^q$  the right singular vectors and  $\lambda_1^q, \dots, \lambda_m^q$  the corresponding singular values.

Each column  $\hat{X}_{Q,i}$  of  $\sqrt{n} \cdot \hat{X}_Q$  is given by the formula

$$\hat{X}_{Q,i} = Q^{-1} \sum_{k=1}^r \eta_k^q \cdot \langle QY_i, \hat{u}_k^q \rangle \cdot \hat{u}_k^q, \quad (57)$$

where  $\eta_k^q = s_k^q/\lambda_k^q$  is the ratio of the new and old singular values. To see this, observe that we can write the  $i^{\text{th}}$  column of the matrix  $\sqrt{n} \cdot Y^q$  as:

$$QY_i = \sum_{k=1}^m \lambda_k^q \cdot \hat{u}_k^q \cdot \hat{v}_{ik}^q, \quad (58)$$

and so by the orthogonality of  $\hat{u}_k^q$ ,  $\hat{v}_{ik}^q = \langle QY_i, \hat{u}_k^q \rangle / \lambda_k^q$ . Consequently, when  $\hat{X}_Q$  is obtained from  $Y^q$  by singular value shrinkage with singular values  $s_1^q, \dots, s_r^q$ , followed by multiplication with  $Q^{-1}$ , we obtain formula (57).

## 4.2 Relation between singular value shrinkage and linear prediction

In this section, we show that for any bounded, symmetric, invertible transformation  $Q$ , the predictor (57) resulting from applying  $Q$  to  $Y$ , shrinking the matrix  $QY$ , and applying  $Q^{-1}$ , converges to a linear predictor of  $X_i$  in the  $\gamma = 0$  limit. In Section 4.3, we deduce from this that when  $Q = H$  is the homogenization transformation, the convergence is to the *optimal* linear filter; when  $Q = I$ , i.e. ordinary shrinkage without homogenization is performed, then the convergence is to a strictly suboptimal linear filter. In this sense, homogenization is an optimal change of coordinates in the  $\gamma = 0$  regime.

First, we establish the consistency of covariance estimation in the  $\gamma = 0$  regime:

**Proposition 4.1.** *If  $p_n/n \rightarrow 0$  as  $n \rightarrow \infty$ , and the subgaussian norm of  $QY_i$  can be bounded by  $C$  independently of the dimension  $p$ , then the sample covariance matrix of  $QY_1, \dots, QY_n$  converges to the population covariance  $Q\Sigma_y Q$  in operator norm.*

*Proof.* We first quote the following result, stated as Corollary 5.50 in [29]:

**Lemma 4.2.** *Let  $Y_1, \dots, Y_n$  be iid mean zero subgaussian random vectors in  $\mathbb{R}^p$  with covariance matrix  $\Sigma_y$ , and let  $\epsilon \in (0, 1)$  and  $t \geq 1$ . Then with probability at least  $1 - 2\exp(-t^2 p)$ ,*

$$\text{If } n \geq C(t/\epsilon)^2 p, \text{ then } \|\hat{\Sigma}_y - \Sigma_y\| \leq \epsilon, \quad (59)$$

where  $\hat{\Sigma}_y = \sum_{i=1}^n Y_i Y_i^\top / n$  is the sample covariance, and  $C$  is a constant.

We also state the well-known consequence of the Borel-Cantelli Lemma:

**Lemma 4.3.** *Let  $A_1, A_2, \dots$  be a sequence of random numbers, and let  $\epsilon > 0$ . Define:*

$$\mathcal{A}_n(\epsilon) = \{|A_n| > \epsilon\}. \quad (60)$$

*If for every choice of  $\epsilon > 0$  we have*

$$\sum_{n=1}^{\infty} \mathbb{P}(\mathcal{A}_n(\epsilon)) < \infty, \quad (61)$$

*then  $A_n \rightarrow 0$  almost surely.*

Now take  $t = \epsilon\sqrt{n/Cp}$ ; then  $n \geq C(t/\epsilon)^2 p$ , and  $t \geq 1$  for  $n$  sufficiently large. Consequently,

$$\mathbb{P}(\|\hat{\Sigma}_y - \Sigma_y\| > \epsilon) \leq 2\exp(-t^2 p) = 2\exp(-n\epsilon^2/C), \quad (62)$$

and so the series  $\sum_{n \geq 1} \mathbb{P}(\|\hat{\Sigma}_y - \Sigma_y\| > \epsilon)$  converges, meaning  $\|\hat{\Sigma}_y - \Sigma_y\| \rightarrow 0$  almost surely as  $n \rightarrow \infty$ .

We now need to check that the subgaussian norm of  $Y_i = X_i + \varepsilon_i$  from the spiked model is bounded independently of the dimension  $p$ . But this is easy if the distribution of variances of  $\varepsilon_i$  is bounded, using, for example, Lemma 5.24 of [29].  $\square$

Using Proposition 4.1 and formula (57), we can show the following result. Let  $u_1^q, \dots, u_r^q$  denote the top  $r$  eigenvectors of  $Q\Sigma_y Q$ , and let

$$\hat{X}_{Q,i}^{lin} = \sum_{k=1}^r \eta_k^q \cdot \langle QY_i, u_k^q \rangle \cdot Q^{-1}u_k^q, \quad (63)$$

be a linear filter, where the  $\eta_k^q$  are chosen optimally to minimize the AMSE for each observation. Let

$$\hat{X}_Q^{lin} = [\hat{X}_{Q,1}^{lin}, \dots, \hat{X}_{Q,n}^{lin}] / \sqrt{n}. \quad (64)$$

Then we have:

**Proposition 4.4.** *In the limit  $p/n \rightarrow 0$ , we have:*

$$\lim_{n \rightarrow \infty} \|\hat{X}_Q^{lin} - \hat{X}_Q\|_F^2 = \lim_{n \rightarrow \infty} \frac{1}{n} \sum_{i=1}^n \|\hat{X}_{Q,i}^{lin} - \hat{X}_{Q,i}\|^2 = 0. \quad (65)$$

*In other words, the predictor  $\hat{X}_{Q,i}$  is asymptotically equivalent to the linear predictor  $\hat{X}_{Q,i}^{lin}$ .*

### 4.3 The optimality of homogenization

Applying Proposition 4.4 in the case when  $Q = H$ , this shows that the optimal shrinkage estimator with homogenization is equivalent to the following linear predictor:

$$\hat{X}_i = \hat{X}_{H,i} = \sum_{k=1}^r \eta_k^h \cdot \langle HY_i, u_k^h \rangle \cdot H^{-1} u_k^h, \quad (66)$$

where the  $u_k^h$ 's are the top  $r$  eigenvectors of  $H\Sigma_y H = H\Sigma_x H + I$ , i.e. the eigenvectors of  $H\Sigma_x H$ . However, it is well known (see, e.g. [24]) that the best linear predictor  $\hat{X}_i^{\text{opt}}$  for  $X_i$  given  $Y_i$  is given by:

$$\begin{aligned} \hat{X}_i^{\text{opt}} &= \Sigma_x (\Sigma_x + \Sigma_\varepsilon)^{-1} Y_i \\ &= H^{-1} H \Sigma_x H (H \Sigma_x H + I)^{-1} H Y_i \\ &= H^{-1} \sum_{k=1}^r \frac{\ell_k^h}{\ell_k^h + 1} \langle H Y_i, u_k^h \rangle u_k^h \\ &= \sum_{k=1}^r \eta_k^{\text{opt}} \langle H Y_i, u_k^h \rangle H^{-1} u_k^h, \end{aligned} \quad (67)$$

where  $H\Sigma_x H = \sum_{k=1}^r \ell_k^h u_k^h (u_k^h)^\top$ , and  $\eta_k^{\text{opt}} = \ell_k^h / (\ell_k^h + 1)$ . This is an expression of identical form to (66). Furthermore, since the coefficients  $\eta_k^h$  in (66) are optimal, they must equal the optimal coefficients  $\eta_k^{\text{opt}}$ . In other words, the optimal shrinkage estimators used with homogenization from (66) is asymptotically equivalent to the best linear predictor  $\hat{X}_i^{\text{opt}}$ .

On the other hand, the shrinkage estimator without homogenization must be strictly worse so long as  $\Sigma_\varepsilon$  does not commute with  $\Sigma_x$ , since  $\hat{X}_{Q,i}$  will live in the span of  $u_1^q, \dots, u_r^q$ , which are not the population principal components, and hence  $\hat{X}_{Q,i}$  cannot be equivalent to the best linear predictor.

We have shown:

**Corollary 4.5.** *In the limit  $p/n \rightarrow 0$ , we have:*

$$\lim_{n \rightarrow \infty} \|\hat{X}^{\text{opt}} - \hat{X}\|_F^2 = \lim_{n \rightarrow \infty} \frac{1}{n} \sum_{i=1}^n \|\hat{X}_i^{\text{opt}} - \hat{X}_i\|^2 = 0. \quad (68)$$

Furthermore, for any choice of  $Q$ ,

$$\lim_{n \rightarrow \infty} \|\hat{X} - X\|_F^2 \leq \lim_{n \rightarrow \infty} \|\hat{X}_Q - X\|_F^2, \quad (69)$$

with equality holding if and only if  $Q\Sigma_\varepsilon Q$  commutes with  $Q\Sigma_x Q$ .

## 5 Out-of-sample prediction

Suppose we have computed the vectors  $\hat{u}_1^h, \dots, \hat{u}_r^h$  based on our observed vectors  $Y_1, \dots, Y_n$ , but we now receive a new observation, which we'll denote  $Y_0 = X_0 + \varepsilon_0$ . We could of course form the  $p$ -by- $(n+1)$  sized matrix of all  $Y_0, Y_1, \dots, Y_n$  and recompute the singular vectors  $\hat{u}_k^h$ ; but we might ask instead if there is a way of using the already-computed  $\hat{u}_k^h$ 's to make a prediction for  $X_0$ , using an estimator of the form (57).

Let's be more precise in formulating the problem. We will refer to the observations  $Y_1, \dots, Y_n$  as *in-sample observations*. We are given the  $r$  left singular vectors  $\hat{u}_1^h, \dots, \hat{u}_r^h$  of the homogenized matrix  $Y^h = [Y_1^h, \dots, Y_n^h] / \sqrt{n}$ . We then receive a new, *out-of-sample observation*  $Y_0 = X_0 + \varepsilon_0$  from the same distribution, but independent of the in-sample observations, and our goal is to predict the vector  $X_0$ .

Because singular value shrinkage with noise homogenization applied to the in-sample observations takes the form

$$\hat{X}_i = \sum_{k=1}^r \eta_k \langle H Y_i, \hat{u}_k^h \rangle H^{-1} \hat{u}_k^h, \quad (70)$$

for certain coefficients  $\eta_k$ , we will consider predictors of the out-of-sample  $X_0$  of the same form:

$$\hat{X}_0 = \sum_{k=1}^r \eta_k^o \langle H Y_0, \hat{u}_k^h \rangle H^{-1} \hat{u}_k^h. \quad (71)$$

We wish to choose the coefficients  $\eta_k^o$  to minimize the AMSE,  $\lim_{n \rightarrow \infty} \mathbb{E} \|\hat{X}_0 - X\|^2$ .

Upon initial inspection, it may appear that the optimal coefficients  $\eta_k^o$  should just be equal to the coefficients  $\eta_k$  used for the in-sample observations. However, this is not the case. It was observed in [10] that for the spiked model with white noise (i.e. in the case  $\Sigma_\varepsilon = I_p$ ), the optimal coefficients  $\eta_k^o$  are, in fact, *different* from the coefficients  $\eta_k$ . This surprising phenomenon arises because the new data point  $Y_0$  is drawn independently of the vectors  $\hat{u}_1^h, \dots, \hat{u}_r^h$ . Perhaps more surprising, however, is that the AMSEs for in-sample and out-of-sample prediction are *identical*.

In this section, we will establish the analogous results for the in-sample and out-of-sample predictors (70) and (71). That is, we will derive explicit formulas for the optimal  $\eta_k^o$ , evaluate the resulting AMSE, and show that it is equal to the AMSE for the in-sample prediction problem. The optimal procedure for in-sample prediction is, by definition, identical to singular value shrinkage with noise homogenization, summarized in Algorithm 1. In Algorithm 2, we describe the optimal out-of-sample prediction method.

---

### Algorithm 2 Optimal out-of-sample prediction

---

- 1: **Input:**  $Y_0; \hat{u}_1^h, \dots, \hat{u}_r^h; \lambda_1^h, \dots, \lambda_r^h$
  - 2: **for all**  $k = 1, \dots, r$  **do**
  - 3:   **if**  $\lambda_k^h > 1 + \sqrt{\gamma}$  **then**

$$\ell_k^h = \left[ (\lambda_k^h)^2 - 1 - \gamma + \sqrt{((\lambda_k^h)^2 - 1 - \gamma)^2 - 4\gamma} \right] / 2$$

$$c_k^h = \sqrt{(1 - \gamma/(\ell_k^h)^2) / (1 + \gamma/\ell_k^h)}$$

$$s_k^h = \sqrt{1 - (c_k^h)^2}$$

$$\mu_\varepsilon = \text{tr}(\Sigma_\varepsilon) / p$$

$$\tau_k = (c_k^h)^2 / \left[ \|\Sigma_\varepsilon^{1/2} \hat{u}_k^h\|^2 - (s_k^h)^2 \mu_\varepsilon \right]$$

$$\alpha_k = 1 / ((c_k^h)^2 + (s_k^h)^2 \mu_\varepsilon \tau_k)$$

$$\eta_k^o = \alpha_k \ell_k^h (c_k^h)^2 / (\ell_k^h (c_k^h)^2 + 1)$$
  - 4:   **else if**  $\lambda_k^h \leq 1 + \sqrt{\gamma}$  **then**

$$\eta_k^o = 0$$
  - 5: **Output:**  $\hat{X}_0 = \sum_{k=1}^r \eta_k^o \langle HY_0, \hat{u}_k^h \rangle H^{-1} \hat{u}_k^h$
- 

## 5.1 The optimal coefficients for in-sample prediction

Before deriving the optimal out-of-sample coefficients  $\eta_k^o$ , we will first derive the optimal in-sample coefficients  $\eta_k$ . That is, we will rewrite the optimal shrinkage with noise homogenization in the form (70).

From Section 4.1, the in-sample coefficients  $\eta_k$  are the ratios of the optimal singular values  $s_k$  derived in Section 3.2 and the observed singular values of  $Y^h$ , denoted  $\lambda_1^h, \dots, \lambda_r^h$ . From Proposition 3.1, we know that

$$\lambda_k^h = \sqrt{(\ell_k^h + 1) \left( 1 + \frac{\gamma}{\ell_k^h} \right)}, \quad (72)$$

and from Section 3.2 we know that

$$s_k = \frac{(\ell_k^h)^{1/2} c_k^h \tilde{c}_k}{(c_k^h)^2 + (s_k^h)^2 \mu_\varepsilon \tau_k} = \alpha_k (\ell_k^h)^{1/2} c_k^h \tilde{c}_k, \quad (73)$$

where  $\alpha_k = ((c_k^h)^2 + (s_k^h)^2 \mu_\varepsilon \tau_k)^{-1}$ . Taking the ratio, and using formulas (25) and (26) for  $c_k^h$  and  $\tilde{c}_k$ , we obtain:

$$\eta_k = \frac{s_k}{\lambda_k^h} = \alpha_k \frac{(\ell_k^h)^{1/2} c_k^h \tilde{c}_k}{\sqrt{(\ell_k^h + 1) \left( 1 + \frac{\gamma}{\ell_k^h} \right)}} = \alpha_k \frac{\ell_k^h (c_k^h)^2}{\sqrt{(\ell_k^h + 1) (\ell_k^h + \gamma)}} \sqrt{\frac{(\ell_k^h)^2 + \gamma \ell_k^h}{(\ell_k^h)^2 + \ell_k^h}} = \alpha_k \frac{\ell_k^h (c_k^h)^2}{\ell_k^h + 1}. \quad (74)$$

That is, we have found the optimal in-sample coefficients to be:

$$\eta_k = \frac{1}{(c_k^h)^2 + (s_k^h)^2 \mu_\varepsilon \tau_k} \cdot \frac{\ell_k^h (c_k^h)^2}{\ell_k^h + 1}. \quad (75)$$

In other words, applying the predictor (70) with coefficients (75) to the in-sample data  $Y_1, \dots, Y_n$  is identical to performing optimal singular value shrinkage with noise homogenization to  $Y_1, \dots, Y_n$ .

## 5.2 The optimal coefficients for out-of-sample prediction

In this section, we will derive the optimal out-of-sample coefficients  $\eta_k^o$ . We have a predictor of the form

$$\hat{X}_0 = \sum_{k=1}^r \eta_k^o \langle HY_0, \hat{u}_k^h \rangle H^{-1} \hat{u}_k^h, \quad (76)$$

where  $\hat{u}_k^h$  are the top left singular vectors of the in-sample observation matrix  $Y^h = H[Y_1, \dots, Y_n]/\sqrt{n}$ . We wish to choose the coefficients  $\eta_k^o$  that minimize the asymptotic mean squared error  $\mathbb{E}\|X_0 - \hat{X}_0\|^2$ . First, we can expand the MSE across the different principal components as follows:

$$\begin{aligned} \|X_0 - \hat{X}_0\|^2 &= \sum_{k=1}^r \|\ell_k^{1/2} z_{0k} u_k - \eta_k^o \langle HY_0, \hat{u}_k^h \rangle H^{-1} \hat{u}_k^h\|^2 \\ &\quad + \sum_{k \neq l} \langle \ell_k^{1/2} z_{0k} u_k - \eta_k^o \langle HY_0, \hat{u}_k^h \rangle H^{-1} \hat{u}_k^h, \ell_l^{1/2} z_{0l} u_l - \eta_l^o \langle HY_0, \hat{u}_l^h \rangle H^{-1} \hat{u}_l^h \rangle. \end{aligned} \quad (77)$$

After taking expectations, the cross-terms vanish and we are left with:

$$\mathbb{E}\|X_0 - \hat{X}_0\|^2 = \sum_{k=1}^r \mathbb{E}\|\ell_k^{1/2} z_{0k} u_k - \eta_k^o \langle HY_0, \hat{u}_k^h \rangle H^{-1} \hat{u}_k^h\|^2. \quad (78)$$

Since the sum separates across the  $\eta_k^o$ , we can minimize each summand individually. We write:

$$\begin{aligned} &\mathbb{E}\|\ell_k^{1/2} z_{0k} u_k - \eta_k^o \langle HY_0, \hat{u}_k^h \rangle H^{-1} \hat{u}_k^h\|^2 \\ &= \ell_k + (\eta_k^o)^2 \mathbb{E} \left[ \langle HY_0, \hat{u}_k^h \rangle^2 \|H^{-1} \hat{u}_k^h\|^2 \right] - 2\ell_k^{1/2} \eta_k^o \mathbb{E} \left[ z_{0k} \langle HY_0, \hat{u}_k^h \rangle \langle u_k, H^{-1} \hat{u}_k^h \rangle \right]. \end{aligned} \quad (79)$$

We first deal with the quadratic coefficient in  $\eta$ :

$$\begin{aligned} \langle HY_0, \hat{u}_k^h \rangle^2 \|H^{-1} \hat{u}_k^h\|^2 &= \langle HX_0 + H\varepsilon_0, \hat{u}_k^h \rangle^2 \|H^{-1} \hat{u}_k^h\|^2 \\ &= \left( \langle HX_0, \hat{u}_k^h \rangle^2 + \langle H\varepsilon_0, \hat{u}_k^h \rangle^2 + \langle HX_0, \hat{u}_k^h \rangle \langle H\varepsilon_0, \hat{u}_k^h \rangle \right) \|H^{-1} \hat{u}_k^h\|^2, \end{aligned} \quad (80)$$

and taking expectations, we get:

$$\mathbb{E} \left[ \langle HY_0, \hat{u}_k^h \rangle^2 \|H^{-1} \hat{u}_k^h\|^2 \right] \sim \left( \mathbb{E} \left[ \langle HX_0, \hat{u}_k^h \rangle^2 \right] + 1 \right) \|H^{-1} \hat{u}_k^h\|^2 \sim \left( \ell_k^h (c_k^h)^2 + 1 \right) \left( \frac{(c_k^h)^2}{\tau_k} + (s_k^h)^2 \mu_\varepsilon \right). \quad (81)$$

Now we turn to the linear coefficient in  $\eta$ :

$$\begin{aligned} \ell_k^{1/2} \mathbb{E} \left[ z_{0k} \langle HY_0, \hat{u}_k^h \rangle \langle u_k, H^{-1} \hat{u}_k^h \rangle \right] &= \ell_k^{1/2} \mathbb{E} \left[ z_{0k} \left( (\ell_k^h)^{1/2} z_{0k} c_k^h + \langle H\varepsilon_0, \hat{u}_k^h \rangle \right) \langle u_k, H^{-1} \hat{u}_k^h \rangle \right] \\ &= \frac{\ell_k^h c_k^h \mathbb{E} \left[ \langle u_k, H^{-1} \hat{u}_k^h \rangle \right]}{\|Hu_k\|} \\ &\sim \ell_k^h (c_k^h)^2 \frac{1}{\tau_k}. \end{aligned} \quad (82)$$

Minimizing the quadratic for  $\eta_k^o$ , we get:

$$\begin{aligned} \eta_k^o &= \left( \ell_k^h (c_k^h)^2 \frac{1}{\tau_k} \right) / \left( \left( \ell_k^h (c_k^h)^2 + 1 \right) \left( \frac{(c_k^h)^2}{\tau_k} + (s_k^h)^2 \mu_\varepsilon \right) \right) \\ &= \frac{1}{(c_k^h)^2 + (s_k^h)^2 \mu_\varepsilon \tau_k} \cdot \frac{\ell_k^h (c_k^h)^2}{\ell_k^h (c_k^h)^2 + 1}. \end{aligned} \quad (83)$$



### 5.3 Equality of the AMSEs

Evaluating the out-of-sample error at the optimal out-of-sample coefficients  $\eta_k^o$ , we find the optimal out-of-sample AMSE (where  $\alpha_k = ((c_k^h)^2 + (s_k^h)^2 \mu_\varepsilon \tau_k)^{-1}$ ):

$$\text{AMSE} = \sum_{k=1}^r \left( \ell_k - \frac{(\ell_k^h)^2 (c_k^h)^4}{\ell_k^h (c_k^h)^2 + 1} \frac{1}{\alpha_k \tau_k} \right) = \sum_{k=1}^r \left( \frac{\ell_k^h}{\tau_k} - \frac{(\ell_k^h)^2 (c_k^h)^4}{\ell_k^h (c_k^h)^2 + 1} \frac{1}{\alpha_k \tau_k} \right). \quad (84)$$

The AMSE of the in-sample predictor is:

$$\sum_{k=1}^r \ell_k (1 - (c_k \tilde{c}_k)^2) = \sum_{k=1}^r \frac{\ell_k^h}{\tau_k} \left( 1 - \frac{(c_k^h \tilde{c}_k^h)^2}{\alpha_k} \right) = \sum_{k=1}^r \left( \frac{\ell_k^h}{\tau_k} - \frac{\ell_k^h (c_k^h \tilde{c}_k^h)^2}{\alpha_k \tau_k} \right) \quad (85)$$

To show equality, we therefore need to show:

$$\ell_k^h (c_k^h \tilde{c}_k^h)^2 = \frac{(\ell_k^h)^2 (c_k^h)^4}{\ell_k^h (c_k^h)^2 + 1}. \quad (86)$$

But this follows from the equality of in-sample and out-of-sample AMSEs for the standard spiked model with isotropic noise, established in [10].

Putting together this result with those from Sections 5.1 and 5.2, we have shown:

**Proposition 5.1.** *The optimal in-sample coefficients  $\eta_k$  are given by :*

$$\eta_k = \frac{1}{(c_k^h)^2 + (s_k^h)^2 \mu_\varepsilon \tau_k} \cdot \frac{\ell_k^h (c_k^h)^2}{\ell_k^h + 1}. \quad (87)$$

*The optimal out-of-sample coefficients  $\eta_k^o$  are given by:*

$$\eta_k^o = \frac{1}{(c_k^h)^2 + (s_k^h)^2 \mu_\varepsilon \tau_k} \cdot \frac{\ell_k^h (c_k^h)^2}{\ell_k^h (c_k^h)^2 + 1}. \quad (88)$$

*The AMSEs for in-sample and out-of-sample prediction are identical, and equal to:*

$$\text{AMSE} = \sum_{k=1}^r \left( \frac{\ell_k^h}{\tau_k} - \frac{(\ell_k^h)^2 (c_k^h)^4}{\ell_k^h (c_k^h)^2 + 1} \frac{1}{\alpha_k \tau_k} \right), \quad (89)$$

where  $\alpha_k = ((c_k^h)^2 + (s_k^h)^2 \mu_\varepsilon \tau_k)^{-1}$ .

## 6 Numerical results

In this section we report several numerical results that illustrate the performance of our predictor in the spiked model, as well as several beneficial properties of homogenization. The code for these experiments will be made available online at <https://github.com/w1eeb/hom-shr>.

### 6.1 Comparison to the best linear predictor

In this experiment, we compared our predictor to the best linear predictor (BLP), defined in equation (67). The BLP is an oracle method, as it requires knowledge of the population covariance  $\Sigma_x$ , which is not accessible to us. However, Proposition 4.4 and Corollary 4.5 predict that as  $p/n \rightarrow 0$ , the optimal shrinkage with homogenization predictor will behave identically to the BLP.

In the same experiments, we also compare our method to OptShrink [26], the optimal singular value shrinker without any transformation. Proposition 4.4 and Corollary 4.5 predicts that as  $p/n \rightarrow 0$ , OptShrink will behave identically to a suboptimal linear filter.

In these tests, we fixed a dimension equal to  $p = 100$ , and let  $n$  grow. Each signal was rank 3, with PCs chosen so that the first PC was a completely random unit vector, the second PC was set to zero on the first  $p/2$  coordinates and random on the remaining coordinates, and the third PC was completely random on the first  $p/2$  coordinates and zero on the remaining coordinates. The signal random variables  $z_{ik}$  were chosen to be Gaussian.

The noise covariance matrix  $\Sigma_\varepsilon$  was generated by taking equally spaced values between 1 and a specified condition number  $\kappa > 1$ , and then normalizing the resulting vector of eigenvalues to be a unit vector. This normalization was done so that in each test, the total energy of the noise remained constant.

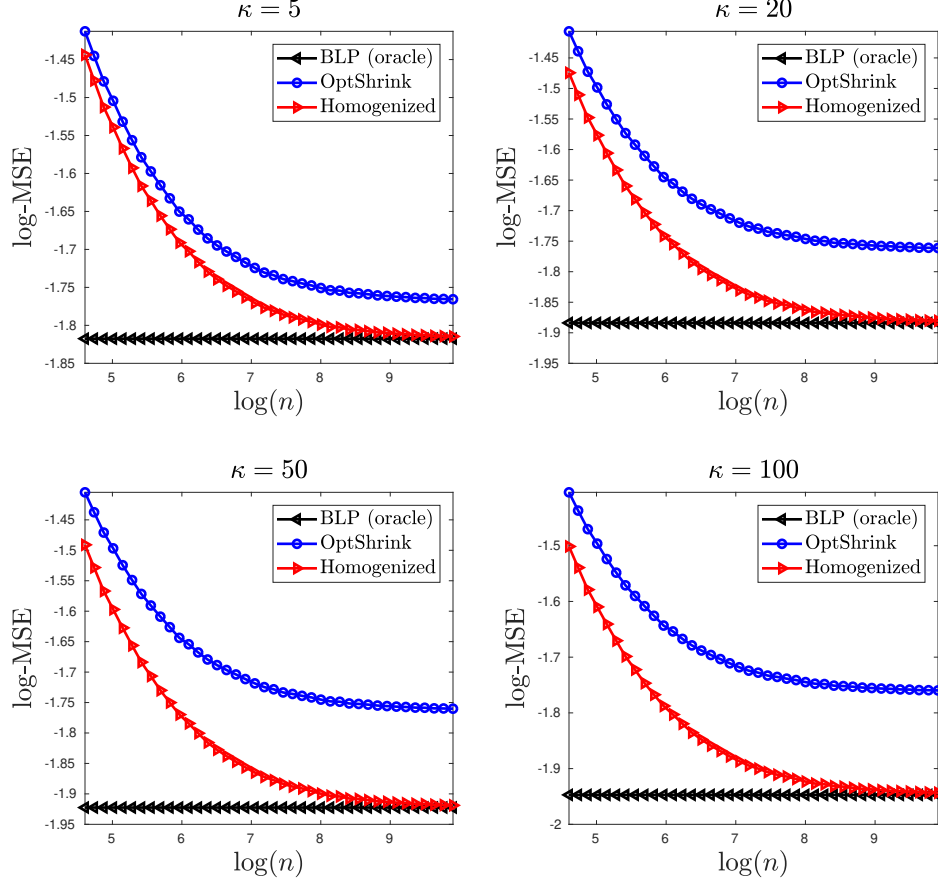


Figure 1: Prediction errors for the optimal homogenized shrinker, the optimal unhomogenized shrinker (OptShrink), and the best linear predictor (an oracle method).

In Figure 1, we plot the average prediction errors as a function of  $n$  for the three methods, for different condition numbers  $\kappa$  of the noise covariance  $\Sigma_\varepsilon$ . The errors are averaged over 500 runs of the experiment, with different draws of signal and noise. As expected, the errors for optimal shrinkage with homogenization converge to those of the oracle BLP, while the errors for OptShrink appear to converge to a larger value, namely the error of the suboptimal linear filter it converges to.

In Figure 2, we plot the results from a similar experiment, though now we display the errors as a function of increasing condition number, for fixed values of  $\gamma = p/n$ . Here,  $p = 200$  was fixed, and we averaged over 50 runs for each test. Again, we see that as the condition number grows, the relative performance of optimal shrinkage with homogenization grows better relative to OptShrink. Furthermore, for larger  $n$  (i.e. small  $\gamma$ ) the performance of optimal shrinkage with homogenization approaches that of the oracle BLP.

## 6.2 Numerical comparison of the angles

The error achievable by any shrinkage method is determined by the angles between the empirical vectors of the prediction matrix and the population singular vectors of the true matrix  $X$ . In this section, we examine the angles between the spanning vectors  $\hat{u}_k$  and  $\hat{v}_k$  of  $\hat{X}$  and, respectively, the population vectors  $u_k$  and  $v_k$ . We show that these angles are smaller (or equivalently, their cosines are larger) than the corresponding angles between the population  $u_k$  and  $v_k$  and the singular vectors of the unhomogenized data matrix  $Y$ .

In Figure 3, we plot the cosines as a function of the condition number  $\kappa$  of the noise matrix  $\Sigma_\varepsilon$ . In this experiment, we consider a rank 1 signal model for simplicity, with a uniformly random PC. We used dimension  $p = 500$ , and drew  $n = 1000$  observations. For each condition number  $\kappa$  of  $\Sigma_\varepsilon$ , we generate  $\Sigma_\varepsilon$  as described in Section 6.1. For each test, we average the cosines over 50 runs of the experiment

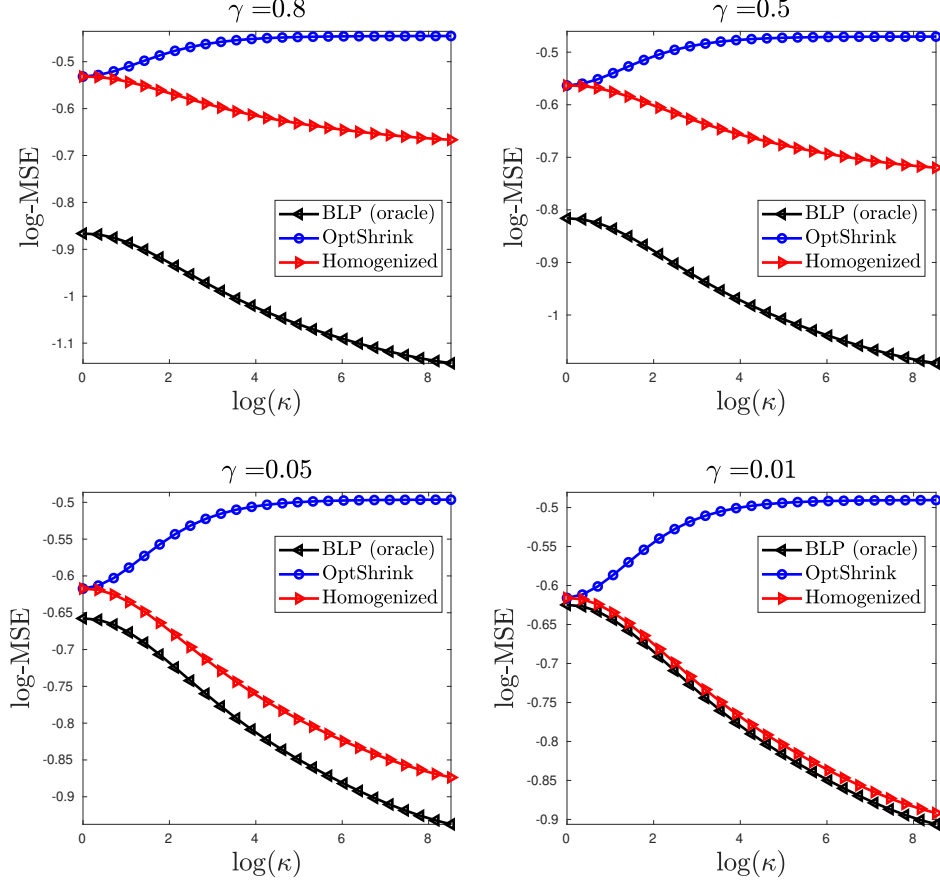


Figure 2: Comparison of homogenized shrinkage, OptShrink, and the best linear predictor as a function of the noise covariance matrix's condition number  $\kappa$ .

(drawing new signals and new noise each time). Both signal and noise are Gaussian. We plot both the cosines themselves, and the ratio between the cosines.

As we see, the cosines improve dramatically after homogenization. As  $\kappa$  grows, i.e. the noise becomes more heteroskedastic, the improvement becomes more pronounced. We emphasize that for the PCs, we are comparing the vectors  $\hat{u}_k$  to  $u_k$ ; that is, we compute the left singular vectors  $\hat{u}_k^h$  of  $Y^h$ , and then unhomogenize them to produce  $\hat{u}_k = H^{-1}\hat{u}_k^h/\|H^{-1}\hat{u}_k^h\|$ ; it is these latter vectors that span the left singular subspace  $\hat{X}$ , and so it is these that we compare to the  $u_k$ .

From Proposition 3.4, we know that after homogenization the operator norm of the signal matrix increases relative to the noise matrix. We would therefore expect the singular vectors of  $Y^h$  to move closer to those of  $X^h$ ; that is, homogenization has a denoising effect on the singular vectors and improves the subspace estimation.

### 6.3 Comparing in-sample and out-of-sample prediction

In this next experiment, we compare the performance of in-sample and out-of-sample prediction, as described in Section 5. Optimal in-sample prediction is identical to performing optimal singular value shrinkage with noise homogenization to the in-sample data  $Y_1, \dots, Y_n$ . For out-of-sample prediction, we use the expression of the form (71) with the optimal coefficients  $\eta_k^o$  from Proposition 5.1.

We ran the following experiments. For a fixed dimension  $p$ , we generated a random value of  $n > p$ . We then chose three random PCs from the same model described in Section 6.1, and we generated pools of  $n$  in-sample and out-of-sample observations. We performed optimal shrinkage with homogenization on the in-sample observations, and applied the out-of-sample prediction to the out-of-sample data using the vectors  $\hat{u}_k^h$  computed from the in-sample data. We then computed the MSEs for the in-sample and out-of-sample data matrices. This whole procedure was repeated 2000 times.

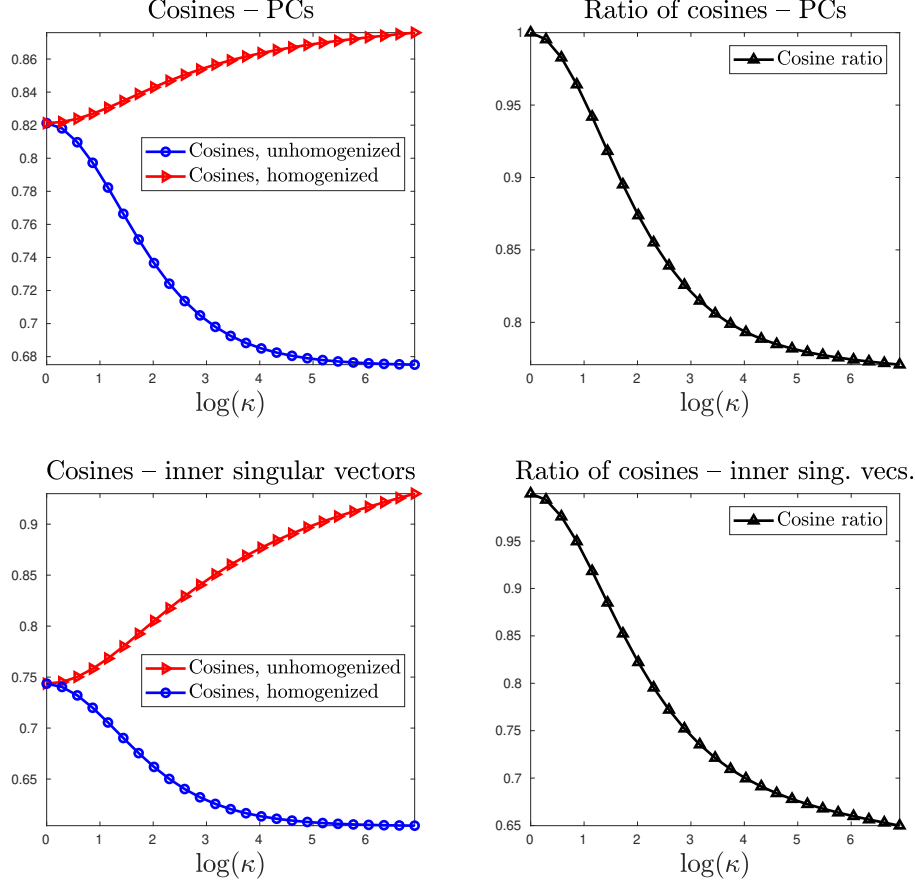


Figure 3: Comparison of the cosines between the empirical and population singular vectors, for the raw data and the homogenized data, as a function of the noise covariance matrix’s condition number  $\kappa$ .

In Figure 4, we show scatterplots of the in-sample and out-of-sample predictions for  $p = 50$  and  $p = 500$ . In both plots, we see that there is not a substantial difference between the in-sample and out-of-sample prediction errors, validating the asymptotic prediction made by Proposition 5.1. Even for the low-dimension of  $p = 50$ , there is very close agreement between the performances, and for  $p = 500$  they perform nearly identically.

## 6.4 Signal detection and rank estimation

In this experiment, we show that homogenization improves signal detection. We generated data from a rank 1 model, with a weak signal. We computed all the singular values of the original data matrix  $Y$ , and the homogenized matrix  $Y^h$ . In Figure 5, we plot the the top 20 singular values for each matrix.

It is apparent from the comparison of these figures that the top singular value of the homogenized matrix pops out from the bulk of noise singular values, making detection of the signal component very easy in this case. By contrast, the top singular value of the raw, unhomogenized matrix  $Y^h$  does not stick out from the bulk. Proposition 3.4 would lead us to expect this type of behavior, since the signal matrix increases in strength relative to the noise matrix.

## 7 Conclusions and future work

We have derived the optimal singular value shrinkage method for prediction in the spiked model with heteroskedastic noise, where the data is homogenized before shrinkage, and unhomogenized after shrinkage. We also showed the in that  $\gamma = 0$  regime, optimal shrinkage with homogenization converges to the best linear predictor, whereas optimal shrinkage without homogenization converges to a suboptimal linear

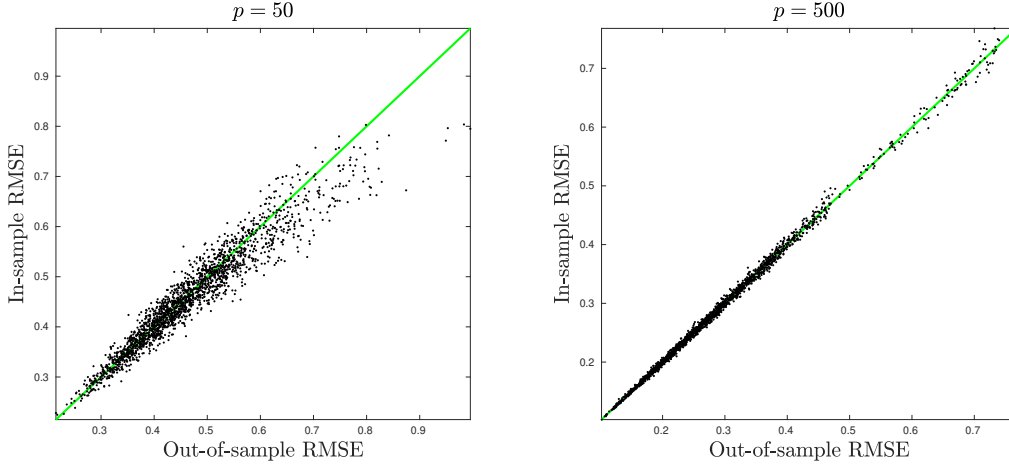


Figure 4: Comparison of in-sample and out-of-sample denoising for  $p = 50$  and  $p = 500$ .

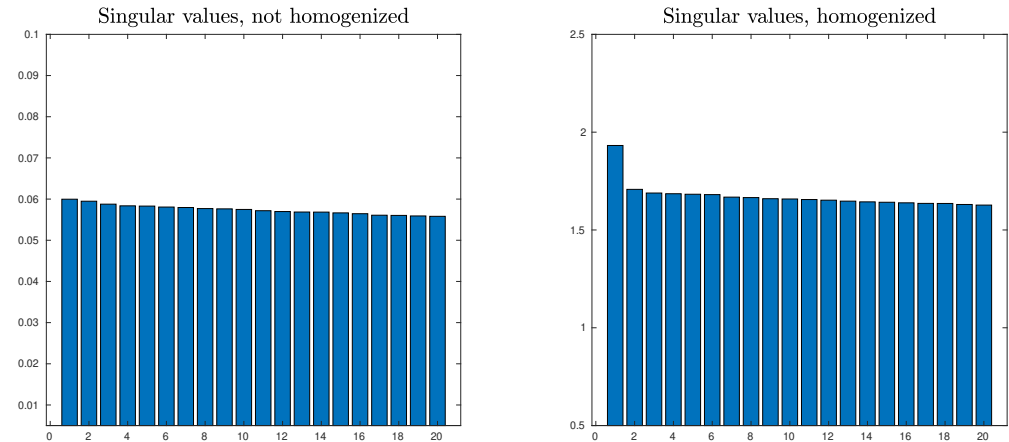


Figure 5: The top 20 empirical singular values of the raw data matrix  $Y$  and the homogenized data matrix  $Y^h$ , for a rank 1 signal.

filter. We showed that the operator norm SNR of the observations increases after homogenization. We also extended the analysis on out-of-sample prediction found in [10] to the homogenization procedure.

There are a number of potentially interesting directions for future research. First, while previous works have employed similar procedures of shrinkage plus homogenization, they used suboptimal shrinkers. It would be of interest to revisit these works with the optimal shrinkers, and determine how much of an improvement is achieved with the more principled choice we have derived.

Our current analysis is restricted to the setting of Gaussian noise. In future work, we will try to extend the analysis to more general noise matrices. This likely requires a deeper understanding of the distribution of the projection of the empirical singular vectors onto the orthogonal complement of the population signal vectors in the setting of non-Gaussian noise.

Finally, it is of great interest to understand precisely why the empirical vectors produced by homogenization are so much closer to the population singular vectors than are the empirical singular vectors of the unhomogenized data matrix. This is the subject of ongoing investigation.

## Acknowledgements

The authors would like to thank Edgar Dobriban, Matan Gavish, and Amit Singer for stimulating discussions related to this work. WL acknowledges support from the Simons Foundation Collaboration on Algorithms and Geometry and the NSF BIGDATA program, IIS 1837992. ER acknowledges support from Israeli Science Foundation grant number 1523/16.

## References

- [1] Joakim Andén and Amit Singer. Factor analysis for spectral estimation. In *Sampling Theory and Applications (SampTA), 2017 International Conference on*, pages 169–173. IEEE, 2017.
- [2] Joakim Andén and Amit Singer. Structural variability from noisy tomographic projections. *SIAM Journal on Imaging Sciences*, 11(2):1441–1492, 2018.
- [3] Zhidong Bai and Jack W Silverstein. *Spectral analysis of large dimensional random matrices*. Springer Series in Statistics. Springer, 2009.
- [4] Florent Benaych-Georges, Alice Guionnet, and Mylène Maida. Fluctuations of the extreme eigenvalues of finite rank deformations of random matrices. *Electronic Journal of Probability*, 16:1621–1662, 2011.
- [5] Florent Benaych-Georges and Raj Rao Nadakuditi. The singular values and vectors of low rank perturbations of large rectangular random matrices. *Journal of Multivariate Analysis*, 111:120–135, 2012.
- [6] Tejal Bhamre, Teng Zhang, and Amit Singer. Denoising and covariance estimation of single particle cryo-EM images. *Journal of Structural Biology*, 195(1):72–81, 2016.
- [7] Timothy A. Brown. *Confirmatory factor analysis for applied research*. Guilford Publications, 2014.
- [8] Andreas Buja and Nermin Eyuboglu. Remarks on parallel analysis. *Multivariate Behavioral Research*, 27(4):509–540, 1992.
- [9] Edgar Dobriban. Factor selection by permutation. *arXiv preprint arXiv:1710.00479*, 2017.
- [10] Edgar Dobriban, William Leeb, and Amit Singer. Optimal prediction in the linearly transformed spiked model. *arXiv preprint arXiv:1709.03393v2*, 2018.
- [11] Edgar Dobriban and Art B. Owen. Deterministic parallel analysis. *arXiv preprint arXiv:1711.04155*, 2017.
- [12] David L Donoho, Matan Gavish, and Iain M Johnstone. Optimal shrinkage of eigenvalues in the spiked covariance model. *Annals of Statistics*, 46(6), 2018.
- [13] Matan Gavish and David L. Donoho. Minimax risk of matrix denoising by singular value thresholding. *The Annals of Statistics*, 42(6):2413–2440, 2014.
- [14] Matan Gavish and David L. Donoho. The optimal hard threshold for singular values is  $4/\sqrt{3}$ . *IEEE Transactions on Information Theory*, 60(8):5040–5053, 2014.
- [15] Matan Gavish and David L. Donoho. Optimal shrinkage of singular values. *IEEE Transactions on Information Theory*, 63(4):2137–2152, 2017.
- [16] Gene H. Golub and Charles F. Van Loan. *Matrix Computations*, volume 3. JHU Press, 2012.
- [17] John L. Horn. A rationale and test for the number of factors in factor analysis. *Psychometrika*, 30(2):179–185, 1965.
- [18] J. Edward Jackson. *A user’s guide to principal components*, volume 587. John Wiley & Sons, 2005.
- [19] Iain M Johnstone. On the distribution of the largest eigenvalue in principal components analysis. *Annals of Statistics*, 29(2):295–327, 2001.
- [20] Ian Jolliffe. *Principal component analysis*. Wiley Online Library, 2002.
- [21] Julie Josse and François Husson. Selecting the number of components in principal component analysis using cross-validation approximations. *Computational Statistics & Data Analysis*, 56(6):1869–1879, 2012.
- [22] Shira Kritchman and Boaz Nadler. Determining the number of components in a factor model from limited noisy data. *Chemometrics and Intelligent Laboratory Systems*, 94(1):19–32, 2008.
- [23] Lydia T. Liu, Edgar Dobriban, and Amit Singer. ePCA: High dimensional exponential family PCA. *arXiv preprint arXiv:1611.05550*, 2016.
- [24] D.J.C. MacKay. Deconvolution. In *Information Theory, Inference and Learning Algorithms*, pages 550–551. Cambridge University Press, Cambridge, UK, 2004.
- [25] Brian E. Moore, Raj Rao Nadakuditi, and Jeffrey A. Fessler. Improved robust PCA using low-rank denoising with optimal singular value shrinkage. In *Statistical Signal Processing (SSP), 2014 IEEE Workshop on*. IEEE, 2014.

- [26] Raj Rao Nadakuditi. Optshrink: An algorithm for improved low-rank signal matrix denoising by optimal, data-driven singular value shrinkage. *IEEE Transactions on Information Theory*, 60(5):3002–3018, 2014.
- [27] Debashis Paul. Asymptotics of sample eigenstructure for a large dimensional spiked covariance model. *Statistica Sinica*, 17(4):1617–1642, 2007.
- [28] Andrey A. Shabalin and Andrew B. Nobel. Reconstruction of a low-rank matrix in the presence of Gaussian noise. *Journal of Multivariate Analysis*, 118:67–76, 2013.
- [29] Roman Vershynin. Introduction to the non-asymptotic analysis of random matrices. *arXiv preprint arXiv:1011.3027*, 2010.
- [30] Svante Wold, Kim Esbensen, and Paul Geladi. Principal component analysis. *Chemometrics and Intelligent Laboratory Systems*, 2(1–3):37–52, 1987.
- [31] Luc Wouters, Hinrich W. Göhlmann, Luc Bijnens, Stefan U. Kass, Geert Molenberghs, and Paul J. Lewi. Graphical exploration of gene expression data: a comparative study of three multivariate methods. *Biometrics*, 59(4):1131–1139, 2003.
- [32] H. Henry Yue and Masayuki Tomoyasu. Weighted principal component analysis and its applications to improve FDC performance. In *Decision and Control, 43rd IEEE Conference on*, volume 4. IEEE, 2004.
- [33] Anru Zhang, T. Tony Cai, and Yihong Wu. Heteroskedastic PCA: Algorithm, optimality, and applications. *arXiv preprint arXiv:1810.08316*, 2018.